

Formation and Behavior of Fluorescent Lewis Acid–Base Exciplexes and Triplexes between 3-Aminostilbenes and Aliphatic Amines

Frederick D. Lewis,* Rajdeep S. Kalgutkar, and Todd L. Kurth

Department of Chemistry, Northwestern University, Evanston, Illinois 60208-3113

Received: September 12, 2003; In Final Form: December 2, 2003

The excited singlet states of *trans*-3-aminostilbene and its *N*-methyl derivatives are strongly fluorescent in cyclohexane solution and have large singlet state dipole moments. Addition of low concentrations of alkylamines results in a continuous red shift of the emission maximum and decreasing fluorescence intensity. Analysis of the fluorescence behavior using a combination of singular value decomposition with self-modeling and kinetic analysis provides evidence for the sequential formation of a 1:1 complex (exciplex) and 1:2 complex (triplex) between the excited stilbene and ground state alkylamine, both of which are strongly fluorescent. Both the formation and decay of the exciplex and triplex are dependent upon the extent of amine *N*-alkylation, primary amines forming the most stable exciplex and triplex. Similarly, *N*-aminoalkyl derivatives of the aminostilbenes form intramolecular exciplexes that in turn form 1:1 complexes with added amines. Addition of diaminoalkanes to the aminostilbenes results in sequential formation of 1:1 and 1:2 complexes rather than the formation of a triplex with a single molecule of the diaminoalkanes. Excited state complex formation is attributed to a Lewis acid–base interaction between the excited stilbene (lone pair acceptor) and ground state amine (lone pair donor). An alternative explanation for the red-shifted emission based on Suppan's theory of solvent dielectric enrichment is found to be incompatible with the experimental results.

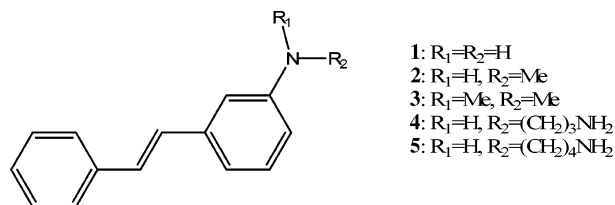
Introduction

The interactions of excited state aromatic molecules with ground state tertiary aliphatic amines have been extensively investigated.^{1–8} Both inter- and intramolecular interactions involving tertiary aliphatic amines can result in the formation of fluorescent, charge-transfer (CT) stabilized exciplexes that possess large dipole moments.^{2–6,9} Exciplex stability increases with decreasing amine ionization potential and is relatively insensitive to steric effects. Experimental and computational studies of arene–amine exciplexes indicate that they exist in shallow conformational minima in which the amine lone pair overlaps nonspecifically with the delocalized arene π^* -orbitals.⁵ Interactions of singlet arenes with secondary or primary amines results in the formation of nonfluorescent exciplexes, primary amines being less reactive as a consequence of their higher ionization potentials.

Some exciplexes have been observed to interact with a second ground state molecule to form a termolecular complex.^{10,11} The use of a strong donor or acceptor results in the formation of a CT stabilized triplex or “exterplex” species. Chandross reported that the intramolecular naphthalene–trialkylamine exciplex can interact with small polar molecules such as propionitrile or dimethylformamide in nonpolar solvents to form stoichiometric fluorescent complexes.⁹ Fluorescence quenching of molecules with intramolecular charge-transfer (ICT) excited states and arene–amine exciplexes by ground state amines correlates with the nucleophilicity of the amines rather than their ionization potentials.^{12–15} The interactions between excited state lone pair acceptors and ground state donors have received far less attention than have CT interactions.

We recently reported that interaction of the singlet state of 3-aminostilbene with ground state primary, secondary, and tertiary aliphatic amines in nonpolar solvents results in the sequential formation of fluorescent, stoichiometric 1:1 and 1:2

CHART 1



complexes.¹⁶ Complex formation in nonpolar solvents and the absence of a correlation of complex stability with amine ionization potential led us to suggest that these complexes are stabilized by lone pair donor–acceptor or Lewis acid–base (LAB) interactions. We report here the results of a detailed investigation of the formation and behavior of both inter- and intramolecular LAB exciplex and triplex species formed upon the reaction of the aminostilbenes **1–3** and their *N*-aminoalkyl derivatives **4** and **5** (Chart 1) with primary, secondary, and tertiary aliphatic amines and with α,ω -diaminoalkanes. The overlapping fluorescence spectra of the monomer, exciplex, and triplex have been deconvoluted and the kinetics of their formation and decay have been resolved using singular value decomposition with self-modeling (SVD-SM) followed by kinetic analysis.^{17,18} The results of this study provide the basis for an explicit structural model for the exciplex and triplex species.

Experimental Section

Synthesis of 1–3. *m*-Nitrobenzaldehyde (Aldrich) was reacted with triphenylphosphonium chloride (Aldrich) in a CH_2Cl_2 – H_2O (50% in K_2CO_3) dual phase system using tetrabutylammonium iodide (Aldrich) as a phase-transfer catalyst (10 mol %).¹⁹ The reaction mixture was stirred at room-temperature overnight under a N_2 atmosphere. After completion of the

reaction, the CH_2Cl_2 layer was washed with water several times and then dried with potassium carbonate. The *trans-m*-nitrostilbene isomer was enriched by refluxing the resulting *cis-trans* mixture in benzene with a catalytic amount of I_2 prior to chromatography. Purification was carried out by column chromatography (SiO_2 /hexanes–ethyl acetate (80:20), 230–400 mesh SiO_2) to remove the *cis* isomer. The *trans* isomer was further purified by recrystallization from MeOH, providing a pale yellow solid in 40% yield. Reduction of the nitro group to the amino group was carried out by using $\text{Zn}/\text{HCl}-\text{AcOH}$ as the reducing agent,²⁰ affording **1** in 85% yield. Purification of **1** was carried out by recrystallization from HPLC grade MeOH. $\text{Mp} = 119-120\text{ }^\circ\text{C}$, lit. $\text{mp} = 120-121\text{ }^\circ\text{C}$.²¹ $^1\text{H NMR}$ (CDCl_3 , 500 MHz): δ 7.49 (2H, d, $J = 8.0$ Hz), 7.34 (2H, t, $J = 8.0$ Hz), 7.24 (1H, t, $J = 8.0$ Hz), 7.14 (1H, t, $J = 8.0$ Hz), 7.03 (1H, d, $J = 16.0$ Hz) 7.01 (1H, d, $J = 16.0$ Hz), 6.85 (1H, s), 6.60 (1H, d, $J = 8.0$), 6.29 (1H, d, $J = 8.0$ Hz), 3.68 (2H, s). Reaction of **1** with formaldehyde and cyanoborohydride afforded a mixture of **2** and **3**. Separation and purification of **2** and **3** were carried out by column chromatography (SiO_2 /hexanes–ethyl acetate (80:20), 230–400 mesh SiO_2). For **2**: $\text{mp} = 50-52\text{ }^\circ\text{C}$; $^1\text{H NMR}$ (CDCl_3 , 500 MHz) δ 7.50 (2H, d, $J = 8.0$ Hz), 7.34 (2H, t, $J = 8.0$ Hz), 7.24 (1H, t, $J = 8.0$ Hz), 7.17 (1H, t, $J = 8.0$ Hz), 7.13 (1H, d, $J = 16.5$ Hz), 7.04 (1H, d, $J = 16.5$ Hz), 6.89 (1H, d, $J = 8.0$ Hz), 6.75 (1H, s), 6.54 (1H, d, $J = 8.0$ Hz), 3.74 (2H, s), 2.88 (3H, s). For **3**: $\text{mp} = 74.5-76.5\text{ }^\circ\text{C}$, lit. $\text{mp} = 75.5-76.5\text{ }^\circ\text{C}$;²² $^1\text{H NMR}$ (CDCl_3 , 500 MHz) δ 7.53 (2H, d, $J = 8.0$ Hz), 7.36 (2H, t, $J = 8.0$ Hz), 7.25 (2H, t, $J = 8.0$ Hz), 7.10 (2H, s), 6.94 (1H, d, $J = 8.0$ Hz), 6.8 (1H, s), 6.69 (1H, d, $J = 8.0$ Hz), 3.00 (6H, s).

Synthesis of 4 and 5. Preparation of **4** and **5** was via the method of Guillard.²³ *trans-m*-Bromostilbene was prepared and purified, via the method used for the nitro compounds described above, utilizing *m*-bromobenzaldehyde as a starting reagent. One equivalent of *trans-m*-bromostilbene, 2 equiv of *t*-BuONa, 2 mol % of 1,1'-bis(diphenylphosphino)ferrocene (dppf), and 1 mol % of (dppf) $\text{PdCl}_2\cdot\text{CH}_2\text{Cl}_2$ were combined under dry nitrogen. Subsequently, 30 mL of anhydrous dioxane was added, followed by addition via syringe of 3 equiv of either 1,3-diaminopropane or 1,4-diaminobutane. The solution was refluxed overnight and subsequently reduced in volume, quenched with minimal water, and then taken up in CH_2Cl_2 . The organic layer was washed twice with concentrated HCl. The aqueous layers were made strongly basic and extracted with CH_2Cl_2 . The resulting oil was then purified by column chromatography (SiO_2 /ethyl acetate–isopropylamine (95:5), 230–400 mesh SiO_2). Both **4** and **5** were found to have greater than 98.5% *trans* isomer as estimated by GC (typical yields were less than 20%). For **4**: $\text{mp} = 61-64\text{ }^\circ\text{C}$; $^1\text{H NMR}$ (CDCl_3 , 500 MHz) δ 7.50 (2H, d, $J = 8.0$ Hz), 7.34 (2H, t, $J = 8.0$ Hz), 7.24 (1H, t, $J = 8.0$ Hz), 7.16 (1H, t, $J = 8.0$ Hz), 7.07 (1H, d, $J = 16.5$ Hz), 7.03 (1H, d, $J = 16.0$ Hz), 6.87 (1H, d, $J = 8.0$ Hz), 6.75 (1H, s), 6.53 (1H, d, $J = 8.0$ Hz), 3.99 (1H, s), 3.24 (2H, t, $J = 8.0$ Hz), 2.87 (2H, t, $J = 7$ Hz), 1.79 (2H, p, $J = 7.0$ Hz), 1.54 (2H, s). For **5**: $\text{mp} = 73-79\text{ }^\circ\text{C}$; $^1\text{H NMR}$ (CDCl_3 , 500 MHz) δ 7.45 (2H, d, $J = 8.0$ Hz), 7.34 (2H, t, $J = 8.0$ Hz), 7.24 (1H, t, $J = 8.0$ Hz), 7.16 (1H, t, $J = 8.0$ Hz), 7.06 (1H, d, $J = 16.5$ Hz), 7.02 (1H, d, $J = 16.0$ Hz), 6.87 (1H, d, $J = 8.0$ Hz), 6.73 (1H, s), 6.52 (1H, d, $J = 8.0$ Hz), 3.17 (2H, t, $J = 7.0$ Hz), 2.75 (2H, t, $J = 7.0$ Hz), 1.68 (2H, p, $J = 7.0$ Hz), 1.57 (4H, p, $J = 7.0$ Hz), 1.55 (2H, s).

Dielectric Constant and Refractive Index Measurements. HPLC grade cyclohexane was used as the bulk solvent. The alkylamines were obtained in their highest purity from Aldrich

and were distilled, under dry nitrogen, from KOH immediately prior to use. The cyclohexane–amine solutions were prepared via weight. Refractive Index measurements were made by utilizing a Bausch and Lomb Abbe-type refractometer.

Dielectric constant measurements were performed using a GenRad 1658 RLC Digibridge fitted with a Digibridge BNC adapter connected to a two terminal, shielded, stainless steel liquid dielectric cell.²⁴ The dielectric constants C_x and dissipations D of each alkylamine–cyclohexane solvent mixture were measured directly. Using the capacitances (C) of the empty cell C_a , corrected with D , and that of cyclohexane C_s , a cell (C_c) and ground capacitance (C_g) were determined and the dielectric constants were subsequently obtained; see eqs 1–4.²⁵

$$C = \frac{C_x}{1 + D^2} \quad (1)$$

$$C_c = \frac{C_0 - C_a}{\epsilon_0 - \epsilon_a} \quad (2)$$

$$C_g = C_0 - C_a \quad (3)$$

$$\epsilon = \frac{C_s - C_g}{C_c} \quad (4)$$

Spectroscopic Measurements. UV–vis spectra were measured on a Hewlett-Packard 8452A diode array spectrometer using a 1 cm path length quartz cell. Total emission spectra were measured on a SPEX Fluoromax spectrometer. All samples were deaerated for 30 min with dry nitrogen prior to analysis and had less than 0.15 absorbance at the wavelength of excitation. Low-temperature spectra were measured in a Suprasil quartz EPR tube (i.d. = 3.3 mm) using a quartz liquid nitrogen coldfinger dewar at 77 K. Total emission quantum yields were measured by comparing the integrated area under the emission curve at an equal absorbance and the same excitation wavelength as an external standard, 9,10-diphenylanthracene ($\Phi_f = 1.0$ at 298 K in cyclohexane).²⁶ All emission spectra are uncorrected and the estimated error for the quantum yields is $\pm 10\%$.

Fluorescence decays were measured on a Photon Technologies International (PTI) Timemaster stroboscopic detection instrument with a gated hydrogen or nitrogen lamp using a scatter solution to profile the instrument response function.²⁷ Nonlinear, least-squares fitting of the decay curves employed the Levenburg–Marquardt algorithm as described by James et al. and implemented by the Photon Technologies International Timemaster (version 1.2) software.²⁸ Goodness of fit was determined by judging the χ^2 (< 1.3 in all cases), the residuals, and the Durbin–Watson parameter (> 1.6 in all cases). Solutions were degassed under vacuum (< 0.1 Torr) through five freeze–pump–thaw cycles.

Results and Discussion

Intramolecular Complex Formation. The absorption spectra of the *m*-aminostilbenes **1** and **3** have been previously described.^{29,30} In contrast to the parent stilbene and its *p*-amino derivatives, which display a single long-wavelength absorption band, **1** and **3** display a long-wavelength band or shoulder near 340 nm and a more intense band near 300 nm. The appearance of multiple long-wavelength transitions has been attributed to splitting of the lowest singlet state by configuration interaction as a consequence of the loss of symmetry in the *m*-aminostilbenes.³⁰ A similar effect has been reported for *m*-(dimethylamino)benzotrile.³¹ The spectra of the secondary amines **2**, **4**, and

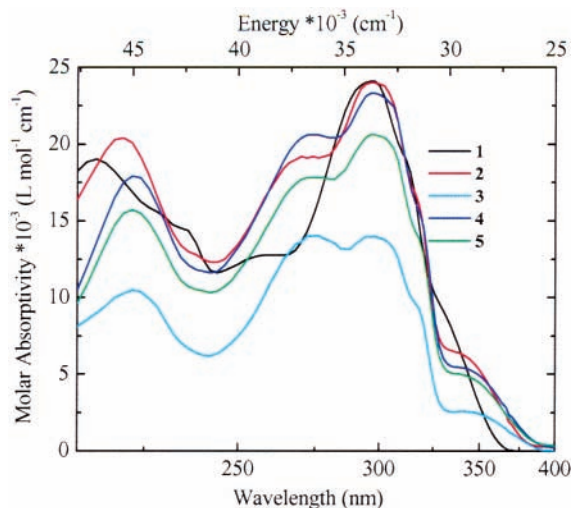


Figure 1. Absorption spectra of **1–5** in cyclohexane solutions, 298 K: **1** (black), **2** (red), **3** (cyan), **4** (blue), **5** (green).

5 are more similar in appearance to that of the primary amine **1** than the tertiary amine **3** (Figure 1). N-Methylation is known to influence the geometry of arylamines, tertiary amines generally having less planar structures than primary or secondary arylamines.³² Changes in geometry are reflected in the oscillator strengths.³³ The absorption maxima of **1–5** (Table 1) are relatively insensitive to solvent polarity, displaying small frequency shifts (<2 nm) in both polar hydroxylic or nonhydroxylic solvents.

The fluorescence spectra of **1** and **3** have also been previously described and consist of a broad band with a shoulder at high frequency, which is more pronounced in the case of **3** vs **1**.^{29,30} The spectrum of **2** is intermediate between those of **1** and **3**, both in terms of band shape and emission maximum (Figure 2). The effects of N-methylation on the appearance of the fluorescence spectra are similar to those for other arylamines.^{31,32} The fluorescence quantum yield for **2** is also intermediate between those reported for **1** and **3**, and its fluorescence lifetime and rate constant are similar to those of **1** (Table 1). The smaller fluorescence rate constant for **3** is consistent with its weaker long-wavelength absorption band.

The fluorescence spectra of **4** and **5** are red-shifted by ca. 1000 cm⁻¹ with respect to those of **2** (Figure 2). Their fluorescence quantum yields are similar to that of **2**; however, their singlet lifetimes are somewhat longer, resulting in smaller fluorescence rate constants. The fluorescence emission and excitation spectra of **2**, **4**, and **5** are similar at 77 K in 2-methyltetrahydrofuran (MTHF) glasses (Figure 3), as are their fluorescence decay times (Table 1). The observation of red-shifted fluorescence in solution but not in a 77 K glass suggests

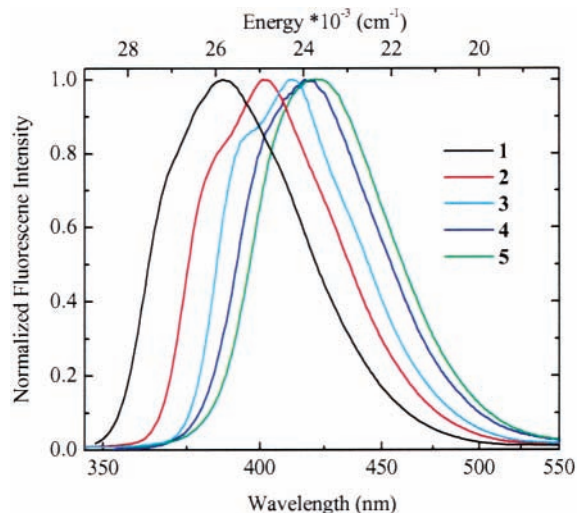


Figure 2. Fluorescence spectra of **1–5** in cyclohexane solutions, 298 K: **1** (black), **2** (red), **3** (cyan), **4** (blue), **5** (green).

that a change in molecular conformation, presumably the formation of an intramolecular complex between the amino-stilbene and the tethered primary amine, is responsible for the red-shifted solution fluorescence of **4** and **5**.

The dipole moments of the ground and excited singlet states of **1** and **3** have been previously reported (Table 1).^{29,30} Ground state dipole moments for **2** and **5** were calculated with PM3/ZINDO as implemented in CAChe.³⁴ Excited state dipole moments can be obtained from the dependence of the fluorescence maxima on the Lippert–Mataga solvent polarity parameter Δf

$$\Delta f = \frac{\epsilon - 1}{2\epsilon + 1} - \frac{n^2 - 1}{2n^2 + 1} \quad (5)$$

where ϵ and n are the solvent dielectric constant and refractive index.³⁵ The solvent dependence of the fluorescence maxima can be described by

$$\nu_{fl} = - \left[\left(\frac{1}{4\pi\epsilon_0} \right) \left(\frac{2}{hca^3} \right) \right] \mu_e (\mu_e - \mu_g) \Delta f + C \quad (6)$$

ϵ_0 is the permittivity of free space, h is Planck's constant, c is the speed of light, a is the cavity radius, μ_e is the relaxed excited state dipole, and μ_g is the ground state dipole. Lippert–Mataga plots for **2** and **5** are shown in Figure 4. As expected, the calculated ground and excited state dipole moments for **2** are similar to those for **1** and **3**. The calculated ground state dipole moment of **5** is somewhat larger than those of **1–3**, plausibly reflecting the influence of the tethered primary amine. The

TABLE 1: Observed and Calculated Spectral Parameters^a

	1	2	3	4	5
λ_{abs}^b , nm	298 (327)	298 (338)	276, 298 (343)	298 (339)	298 (338)
$\log(\epsilon_{max})^b$	4.38 (3.97)	4.38 (3.81)	4.15, 4.15 (3.41)	4.37 (3.73)	4.31 (3.70)
$\lambda_{fl}(298 \text{ K})$, nm	388	401	412	419	423
$\lambda_{fl}(298 \text{ K}, 77 \text{ K})$ (MTHF), nm		445, 426		449, 429	454, 427
Stokes shift ($\times 10^{-3}$) ^c , cm ⁻¹	3.37	3.27	3.21	3.47	3.50
$\tau_f(298 \text{ K}), 77 \text{ K}$, ns	7.5	7.5, 12.1	13.0, 13.0	9.6	12.6, 12.6
Φ_f	0.78	0.74	0.72	0.8	0.71
$10^{-8}k_f$, s ⁻¹	1.04	0.99	0.55	0.83	0.56
μ_g^d (D)	1.5	1.6	1.7		2.9
μ_e^e (D)	11.9	12.5	12.1		10.9, 13.8 ^f

^a 298 K data in cyclohexane and 77 K data in methylcyclohexane unless otherwise noted. ^b Low energy band in parentheses. ^c Calculated by Berlman's method.²⁶ ^d Value calculated using PM3/ZINDO. ^e Calculated using eq 6 and a value of $a = 5$ and 6 \AA for **5**.

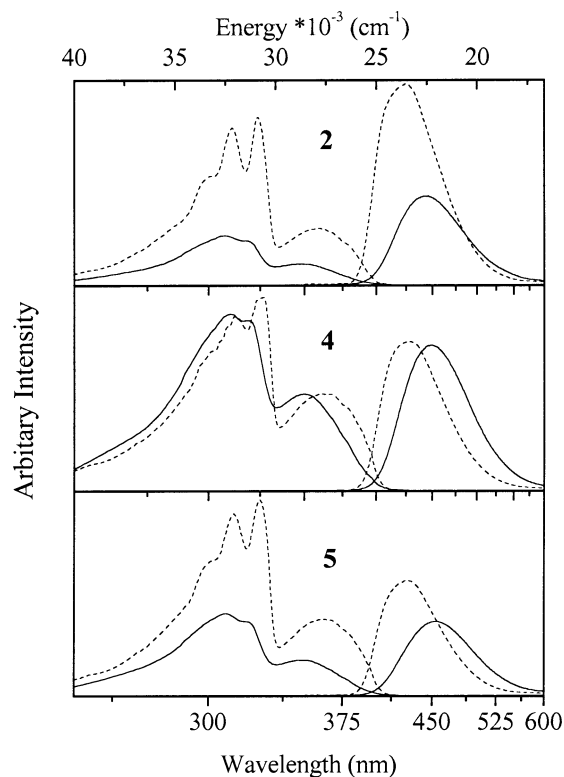


Figure 3. Excitation and emission spectra of **2**, **4**, and **5** in MTHF solutions at 298 K (solid) and 77 K (dash).

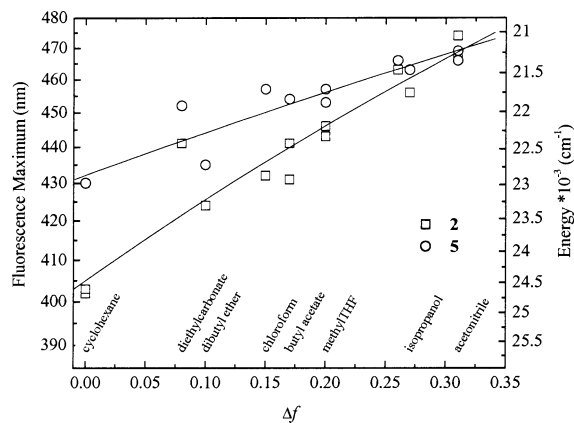


Figure 4. Lippert–Mataga plots for **2** (□) and **5** (○).

smaller slope of the Lippert–Mataga plot for **5** vs **2** results in a smaller excited state dipole moment, if the same cavity radius ($a = 5 \text{ \AA}$)³⁰ is assumed. However, the use of a slightly larger cavity radius (ca. 6 \AA) results in a calculated excited state dipole moment similar to those of **1–3**.

There are numerous reports of the formation of fluorescent ICT exciplexes for tertiary aminoalkylarenes.^{4–6} However, to our knowledge there are no previous reports of the formation of a fluorescent exciplex (either inter- or intramolecular) of a singlet arene with a primary or secondary alkylamine. In addition, the ICT exciplexes formed by tertiary aminoalkylarenes have much larger dipole moments than those observed for **4** or **5**. Both monomer and exciplex fluorescence is observed for CT exciplexes, whereas only a single band is observed for **4** or **5**. Thus the weakly red-shifted emission observed for **4** and **5** in nonpolar solvents cannot be attributed to the formation of a CT stabilized exciplex.

Interaction of Excited Aminostilbenes with Monoamines.

Addition of primary, secondary, or tertiary aliphatic amines to

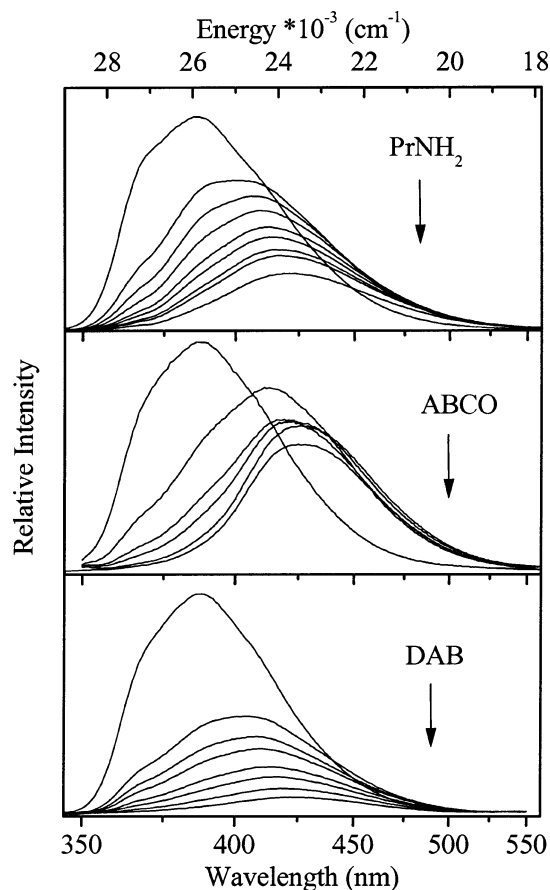


Figure 5. Fluorescence spectra of **1** with PrNH₂, ABCO, and DAB at 298 K, each series having an amine concentration range of 0–250 mM. Added amine results in red-shifted fluorescence.

TABLE 2: Results of SVD-SM and Kinetic Fitting for Cyclohexane Solutions of **1 and **2**^a**

		¹ S*	¹ S*:A	¹ S*:A ₂	k_e	k_{-e}	k_{de}	k_t	k_{-t}	k_{dt}	k_{qt}
		λ_{max}^b	λ_{max}	λ_{max}							
1	PrNH ₂	461	404	424	10	0.13	0.04	7.8	0.38	0.18	0.58
	Pr ₂ NH	439	406	422	11	0.25	0.09	4.0	0.19	0.24	2
	Et ₃ N	441	407	418	8.1	0.1	0.09	0.7	0.05	0.67	0
	ABCO	409	431	411	11	0.04	0.04	2.4	0.01	0.12	0.26
2	DAB	413	439	439	11	0.12	0	2.0	0	0.61	0.29
	PrNH ₂	447	421	430	11	0.01	0.15	0.84	0.07	0.47	0.01
	Pr ₂ NH	437	421	435	11	0.08	0.20	0.32	0.43	0.49	0.10
	Et ₃ N	438	417	429	7.9	0.17	0.14	0.13	0.62	0	0

^a Values are 1×10^{-9} , k_d constrained to equal $\phi_i \tau_i^{-1} = 0.1 \times 10^9$.

^b In pure PrNH₂, Pr₂NH, and Et₃N, respectively.

solutions of **1–3** in nonpolar solvents results in quenching of their fluorescence intensity and a continuous red shift in the fluorescence maxima, as shown for **1** with PrNH₂ and ABCO (azabicyclooctane) in cyclohexane solution in Figure 5. The extent of the red shift, ca. 2000 cm^{-1} , with low concentrations of amine ($<75 \text{ mM}$) is double that observed for the intramolecular complexes formed by **4** or **5**. Diminishing in magnitude, red shifts continue from 75 to 250 mM amine but remain blue-shifted with respect to pure amine solvents (Figure 5, Table 2). Smaller red shifts are observed in moderately polar solvents such as MTHF upon addition of comparable amine concentrations. Fluorescence quenching but no red-shifted emission is observed in more polar solvents; e.g., **2** in acetonitrile and PrNH₂ displays no red shift with increasing amine concentration and yields a linear Stern–Volmer plot with $k_q \tau = K_Q = 3 \times 10^9 \text{ M}^{-1}$.

The appearance of red-shifted emission suggests that the decrease in intensity is not a consequence of straightforward

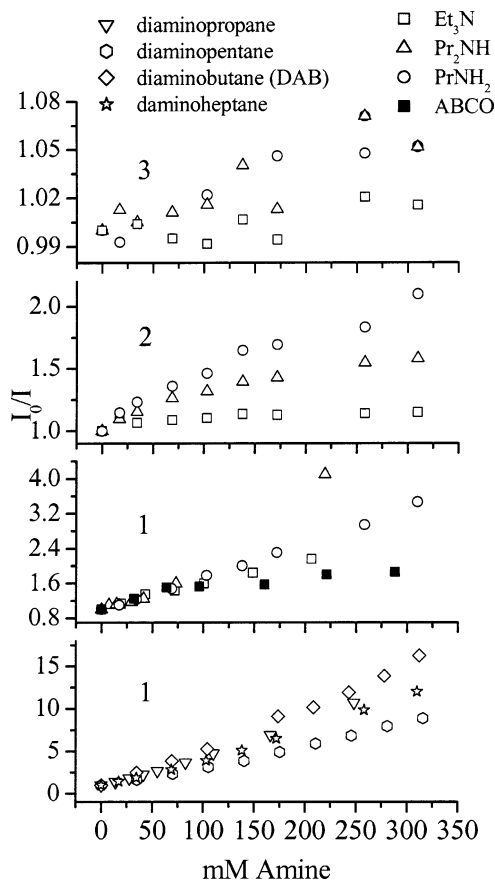


Figure 6. Amine concentration dependence of fluorescence intensity of **1–3** with PrNH₂, Pr₂NH, Et₃N, ABCO, diaminopropane, diaminopentane, diaminobutane (DAB), and diaminoheptane, in cyclohexane.

Stern–Volmer fluorescence quenching of the fluorescent singlet state to the ground state. Non-Stern–Volmer behavior is also evident in plots of the integrated normalized fluorescence intensity (I_0/I) for **1–3** vs amine concentration (Figure 6). The plot for **1** with PrNH₂ displays strong upward curvature, whereas the plots for **1** with Et₃N and for **2** with all three amines display downward curvature. The extent of quenching for a given amine concentration decreases with N-alkylation of both the amino-stilbene (**1** > **2** > **3**) and the alkylamine (PrNH₂ > Pr₂NH > Et₃N). Only slight quenching is observed for **3** with Et₃N (Figure 6). Further evidence for non-Stern–Volmer behavior is provided by the amine concentration dependence of the fluorescence intensities at single wavelengths. As shown in Figure 7 for **1** with PrNH₂, the intensity at 351 nm decreases continuously with increasing PrNH₂ concentration, whereas the intensity at 513 nm increases to a maximum value near 75 mM PrNH₂ and then decreases slowly with PrNH₂ concentration.

The fluorescence decay times for **1** with PrNH₂ also display non-Stern–Volmer behavior. As may be observed in Figure 8, the value of τ determined at 351 nm decreases gradually at amine concentrations below 150 mM, but more precipitously at higher concentrations. The value of τ determined at 513 nm initially increases and then decreases, to a lesser degree than **1**, with added amine. At these wavelengths single exponential fits are satisfactory. At intermediate wavelengths, for each concentration of amine, neither single nor dual exponential fits were satisfactory. Attempts to apply global analysis to resolve multiple lifetimes were unsuccessful. Time-resolved fluorescence spectra for **1** with 150 mM PrNH₂ are shown in Figure 9 along with the steady state spectra of **1** in the absence of amine and with 150 mM PrNH₂. A time-dependent red shift in the

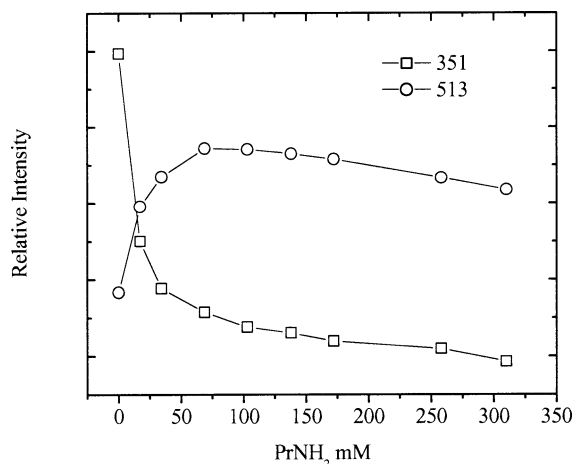


Figure 7. PrNH₂ concentration dependence of the fluorescence intensity of **1** at 513 (○) and 351 nm (□).

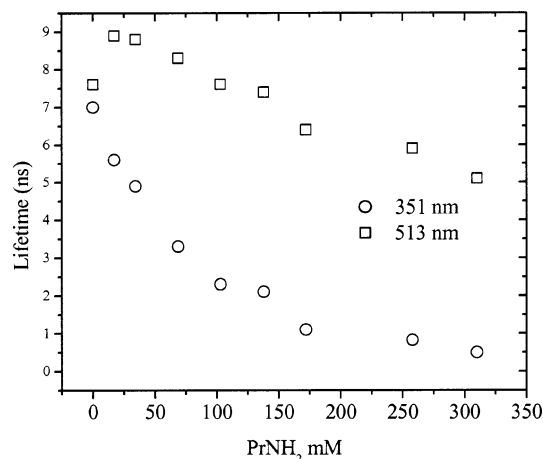


Figure 8. PrNH₂ concentration dependence of the fluorescence lifetime of **1** in cyclohexane solutions, 298 K: 351 nm (○) 513 nm (□).

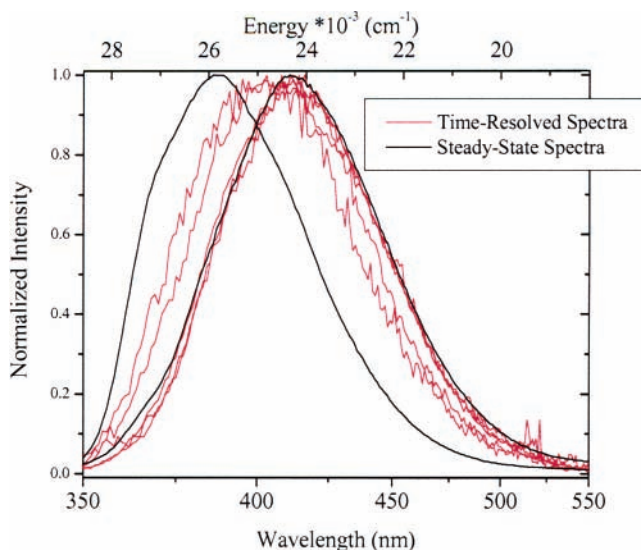


Figure 9. Time-resolved and steady state fluorescence of **1** with PrNH₂ in cyclohexane solutions, 298 K. Steady state spectra, 0 and 150 mM PrNH₂ (black) and time-resolved spectra, 150 mM PrNH₂ (red). Time-resolved delay times are 5, 10, 20, 30, and 40 ns after decay maximum.

entire fluorescence band is observed from a value of 402 nm at short delay times to 412 nm at long delay times. The latter value is similar to the maximum in the steady state fluorescence of **1** with 150 mM PrNH₂.

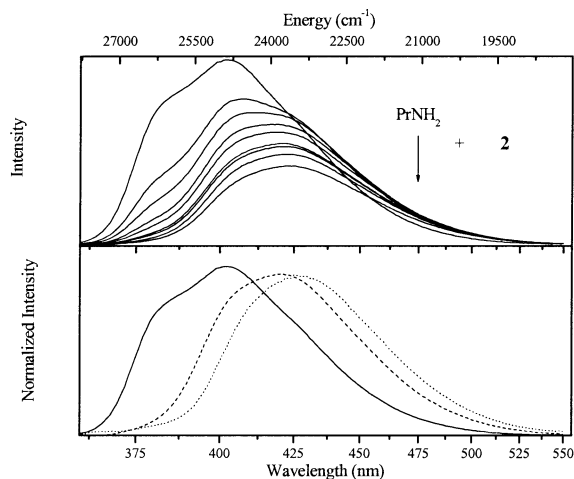


Figure 10. (Top) fluorescence spectra of **2** in cyclohexane solution in the presence of 0–310 mM PrNH₂. Added amine results in red-shifted fluorescence. (Bottom) deconvoluted fluorescence spectra of the monomer (—), exciplex (---), and triplex (···).

Singular Value Decomposition Analysis. A plausible explanation for the effects of added amines on the fluorescence spectra of the aminostilbenes is the sequential formation of one or more excited state complexes. Analysis of the spectral matrixes for the fluorescence with increasing amine concentration by means of SVD-SM indicates the presence of three components. The SVD technique treats the fluorescence spectra as vectors. The spectral vectors form a data matrix (**D**) that may be described by a matrix (**U**) of basis vectors, a diagonal matrix (**S**) of singular values, and a matrix (**V**) consisting of spectral component evolution vectors (eq 7). The relative magnitude of

$$\mathbf{D} = \mathbf{USV}^T \quad (7)$$

the singular values determines the number of basis vectors. The orthogonal basis set of vectors, \mathbf{U}_n , may be linearly combined to form either the original spectral vectors or the unresolved spectral component vectors, \mathbf{C}_j (eq 8). These spectral compo-

$$\mathbf{C}_j = \sum_n a_{n,j} \mathbf{U}_{n,j} \quad (8)$$

nents may be grouped to form the product matrix **N**. To concurrently determine the set of component spectra (**C**) and the set of evolution vectors (**K**), the coefficients ($a_{n,j}$) of the linear combination (eq 9) are determined via a self-modeling

$$\mathbf{K} = \mathbf{N}^{-1}\mathbf{D} \quad (9)$$

(SM) technique.¹⁷ In our application, the SM technique is simply the adherence to spectral nonnegativity of the resulting component and evolution vectors. Via bracketing of errant solutions, uncertainty of the component maxima is similar to that of the instrument, ± 3 nm.

The resultant pure component spectra obtained for **2** with PrNH₂ are shown in Figure 10 and are assigned to the monomer, a 1:1 complex, and a 1:2 complex. Because these complexes are dissociated in the ground state, we refer to them as exciplex and triplex. Emission maxima for the exciplex and triplex (Table 2) are red shifted by ca. 20 and 30 nm, respectively, from that of the monomer (401 nm). The concentration vectors obtained from the SVD analysis of the PrNH₂ spectra are shown in Figure 11. The concentration dependence of the vectors clearly indicates

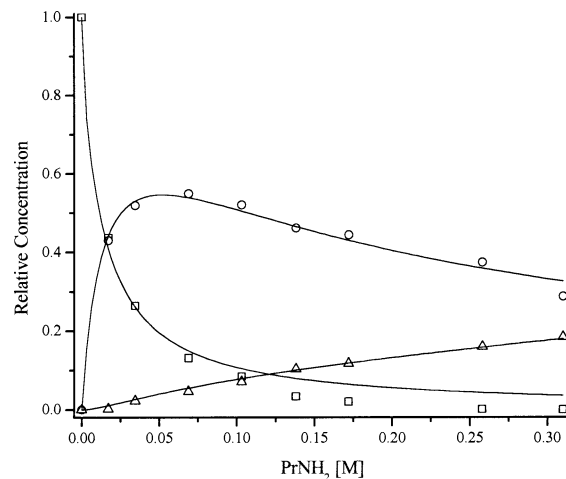
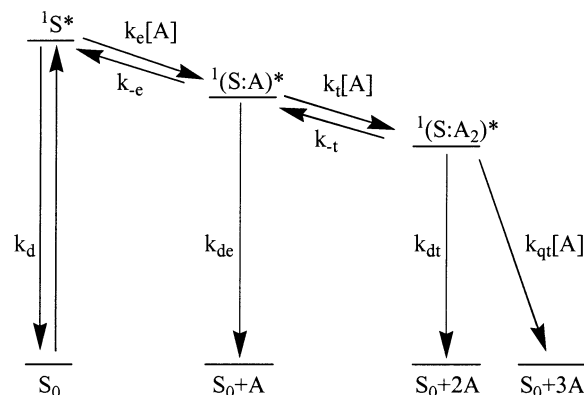


Figure 11. Relative concentrations of **2** (□), exciplex (○), and triplex (△), obtained from SVD-SM of the data in Figure 10. The lines are fits of the data to the model in Scheme 1 corresponding to the parameters in Table 2.

SCHEME 1



that the second and third components are formed sequentially. The growth and decay of the exciplex component is similar to that of the 513 nm fluorescence intensity shown in Figure 7.

Qualitatively similar results are obtained for **1** and **2** with each of the amines studied. The growth of the exciplex component shows similar concentration dependence for all four amines; however, the growth of the triplex is noticeably retarded for Et₃N when compared to the other amines. Three components were also obtained by SVD analysis of the fluorescence spectra of **1** with PrNH₂, Pr₂NH, and Et₃N. The components assigned to exciplex and triplex display somewhat larger red shifts than those for **2** (Table 2). The growth of the triplex is noticeably faster than is the case for **2**, especially in the case of **1** with Et₃N. Addition of amines to **3** causes only small red shifts (<10 nm) in the fluorescence maximum. SVD-SM analysis of these spectra produced only two components which are assigned to **3** and an exciplex.

A kinetic model for reversible sequential formation of the exciplex and triplex and quenching of the triplex by amine is shown in Scheme 1, where k_d , k_{de} , and k_{dt} are the sum of the radiative and nonradiative rates for the monomer, exciplex, and triplex, respectively. Kinetic modeling of the concentration vectors for **1** and **2** with the aliphatic amines using a multistep numerical integration technique provides the rate constants reported in Table 2. Rate constants were optimized using an iterative BFGS quasi-Newton or Nedler–Mead simplex optimization procedure and represent best fits (e.g., Figure 11).³⁶ No attempt was made to model the kinetics for interaction of **3** with amines.

Rate constants for exciplex formation (k_c) for **1** or **2** with PrNH₂ and Pr₂NH and for **1** with ABCO are diffusion limited. The values for Et₃N are slightly slower. Formation of the triplex between **1** and PrNH₂ (k_t) is somewhat slower than exciplex formation. Values of k_t decrease with amine N-alkylation and are significantly slower for **2** than for **1**, and no triplex can be resolved for **3**. The value of k_t for **1** with ABCO is much closer to that of the secondary amine Pr₂NH than that of the tertiary amine Et₃N, plausibly reflecting the decreased steric demand for the bicyclic tertiary amine ABCO.

Rate constants for dissociation of the exciplexes and triplexes (k_{-c} and k_{-t}) are much slower than for their formation; however, assumption of irreversible exciplex formation leads to inferior results for the kinetic modeling. In the case of **1**, unimolecular decay rate constants for the exciplexes (k_{de}) are smaller than those for the monomer ($k_d = \phi_f/\tau_f = 0.1 \times 10^9 \text{ s}^{-1}$) whereas those for the triplexes (k_{dt}) are larger. In the case of **2**, decay of the triplexes is also more rapid than that of the exciplexes. Thus the rate constants for both the formation and decay of the triplexes are sensitive to steric effects, methylation of either the aminostilbene or the aliphatic amine resulting in decreased rate constants for formation and increased rate constants for dissociation or decay. On the basis of the amine concentration dependence of the total fluorescence intensity, it is likely that the exciplex, like the monomer, decays predominantly via fluorescence, whereas nonradiative decay pathways are more important for the triplexes.

The decrease in intensity and decay time for the long-wavelength (513 nm) fluorescence of **1** with Pr₂NH with increasing amine concentration (Figures 7 and 8) indicates that the triplex is quenched by ground state amine. Weak fluorescence is observed for **1–3** in pure alkylamine solvents (Table 2) and is red-shifted with respect to the fluorescence of the triplexes in cyclohexane solution. This might result from either the formation of higher order 1:*n* complexes ($n > 2$) or from a bulk solvent polarity effect on the fluorescence of the monomer or the 1:1 or 1:2 complexes. Because SVD analysis does not indicate the presence of a fourth component, 1:3 and higher order complexes are either nonfluorescent or very weakly fluorescent. Rate constants for quenching of the triplex (k_{qt}) are generally quite small and cannot be resolved for the triplexes of **1** or **2** with Et₃N.

Interaction of Diaminostilbenes with Amines and Aminostilbenes with Diaminoalkanes. Reaction of ground state amines with the excited states of **4** or **5** might be expected to result in the formation of a 1:1 complex between the intramolecular exciplex and the amine. Addition of PrNH₂ to cyclohexane solutions of **5** does in fact result in a decrease in fluorescence intensity and a red shift in the fluorescence maximum. SVD-SM analysis of the fluorescence spectra yields two components with maxima at 423 and 428 nm, which are assigned to the intramolecular exciplex and bimolecular triplex. These values are similar to those for the exciplex and triplex of **2** with PrNH₂ (421 and 430 nm). The evolution vectors were not modeled in this case.

The interaction of singlet **1** with several α,ω -diaminoalkanes results in more efficient quenching of its fluorescence intensity than is the case for interaction with monoamines (Figure 6). The efficiency of quenching is dependent upon the alkane chain length (butyl > propyl > heptyl > pentyl). SVD-SM analysis of the fluorescence spectra obtained for **1** with 1,4-diaminobutane (DAB, Figure 5) indicates the sequential formation of an exciplex and triplex with emission maxima at 413 and 439 nm, respectively. These values are red-shifted in comparison to the

exciplex and triplex of **1** with PrNH₂. However there is no indication that a triplex is formed between **1** and a single molecule of DAB. Similar results were obtained for the other diaminoalkanes.

Kinetic modeling of the concentration vectors for **1** with DAB provides rate constants reported in Table 2. The values for k_c and k_{-c} are similar to those for **1** with PrNH₂; however the value of k_t is smaller for DAB vs PrNH₂ and the value of k_{qt} is larger, suggesting that the triplex formed with DAB is less stable than that formed by PrNH₂.

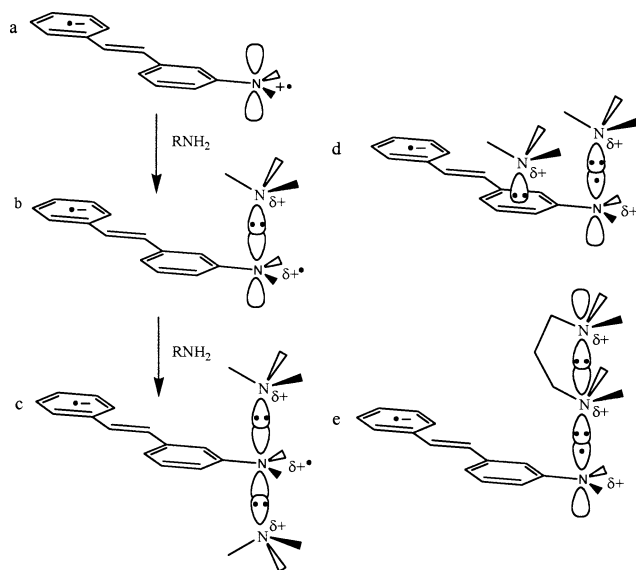
Model for Stoichiometric Complex Formation. The behavior of the excited state complexes formed between the aminostilbenes and ground state amines differs in several important respects from that of the CT-stabilized exciplexes formed between singlet arenes and trialkylamines.^{2,4–6} First, in the case of **1** and **2**, exciplex formation occurs with diffusion controlled rates for primary and secondary amines and slightly slower rates for tertiary amines. Singlet arenes form fluorescent exciplexes with tertiary amines and nonfluorescent exciplexes with secondary or primary amines.⁸ Second, exciplex fluorescence from **1** and **2** is observed only in nonpolar solvents, whereas the stability of arene–amine exciplexes increases with increasing solvent polarity.¹ Third, reaction of the exciplexes of **1** and **2** with a second equivalent of amine results in the formation of fluorescent triplexes, whereas reaction of both inter- and intramolecular arene–amine exciplexes with ground state amines results exclusively in quenching of the exciplex fluorescence.^{12,13,15}

There are also differences in the apparent steric requirements for the formation of the excited state complex of the aminostilbenes and those of CT-stabilized arene–amine exciplexes. The intramolecular exciplexes formed by **4** and **5** have fluorescence maxima similar to that of the intermolecular exciplex formed by **2** with PrNH₂, suggesting that the intra- and intermolecular exciplexes have similar geometries. In contrast, the fluorescence maxima for intramolecular arene–amine exciplexes with tri- or tetramethylene tethers are at higher energy than their intermolecular analogues, presumably due to restrictions on the exciplex geometry by their tethers, which are too short to permit overlap of the nitrogen lone pair orbital with the arene π^* orbital.⁶

These differences suggest that the excited complexes formed by the aminostilbenes differ in structure and electronic character from normal CT-stabilized arene–amine exciplexes. A structural model for the 1:1 and 1:2 complexes formed from the aminostilbenes and amines is shown in Scheme 2. The singlet state of the aminostilbenes (Scheme 2a) is shown as having aniline–styrene CT character, in accord with the moderately large dipole moments of aminostilbenes and other aminoarenes (Table 1).^{30,31} Exciplex formation is shown to require the specific overlap of the amine nonbonded orbital with the electron-deficient π -orbital of the aminostilbene nitrogen (Scheme 2b), and triplex formation requires a specific interaction with the other lobe of the π -orbital (Scheme 2c). Thus we refer to the excited complexes as Lewis acid–base or LAB exciplexes and triplexes, to distinguish them from the better known CT exciplexes.

The proposed model for LAB exciplexes and triplexes (Scheme 2b,c) accounts for both the reactant structure and solvent dependence for these excited state complexes. Increasing alkylation of either the aminostilbene or aliphatic amine nitrogen results in smaller equilibrium constants for LAB complex formation. When both amines are tertiary, no complex formation is detected. In this respect, these excited complexes are similar to the Lewis acid–base complexes formed between ground state

SCHEME 2



amines and Lewis acids such as BF_3 , the stability constants for which decrease in the order $\text{RNH}_2 > \text{R}_2\text{NH} \gg \text{R}_3\text{N}$.³⁷ Delocalization of the positive charge over two or three nitrogens in the excited state is not expected to result in an increase in the CT character of the polar aminostilbene singlet states. In fact, the polarity of the intramolecular LAB exciplex formed by **5** is similar to or smaller than that of the aminostilbene **2** (Table 1). Thus formation of LAB complexes cannot compete with solvation of the aminostilbene singlet state in polar solvents.

Alternative triplex structural models could have both amines interacting with the same face of the aminostilbene (monofacial model, Scheme 2d) or the second amine interacting with the first amine (“exterplex” model, Scheme 2e). The monofacial model is analogous to that proposed for the intramolecular triple complex formed between singlet anthracene and the two equivalent nitrogens of an attached cryptand.¹¹ The exterplex model has been invoked to explain the quenching of arene–amine CT exciplexes by ground state amines and diaminoalkanes.^{15,38} Both of these models would be expected to be favored for diaminoalkane quenchers and thus are inconsistent with the observed sequential formation of 1:1 and 1:2 complexes between singlet **1** and DAB. In addition, formation of an exterplex would be impossible for ABCO, which is observed to form a 1:2 complex more readily than Et_3N (Table 2). The observation of a large value of k_{qt} for the triplex of **1** with DAB suggests that an exterplex-type interaction may be responsible for quenching of the fluorescent triplex. The increased polarity of the local solvent shell of the 1:1 and 1:2 complex, due to the tethered primary amine of the diaminoalkanes, can account for the larger red shift for these complexes vs the complexes formed by monoamines (Table 2).

Alternative Model: Dielectric Enrichment. An alternative explanation for the observation of continuously red-shifted emission upon the addition of amines to solutions of the aminostilbenes is dielectric enrichment of the local solvent shell.^{39,40} Suppan and others have shown that numerous cases of solvent induced emission shifts in binary solvents may be described by a dynamic increase in the local polarity around a solute dipole.^{39,41} In such systems, fluorophores emit at energies much lower than expected in pure solvents of similar polarity. This is also the case for aminostilbene–alkylamine–cyclohexane solutions. As seen in Figure 12, addition of small amounts of amine (<1 mol %) induces a large shift in the aminostilbene

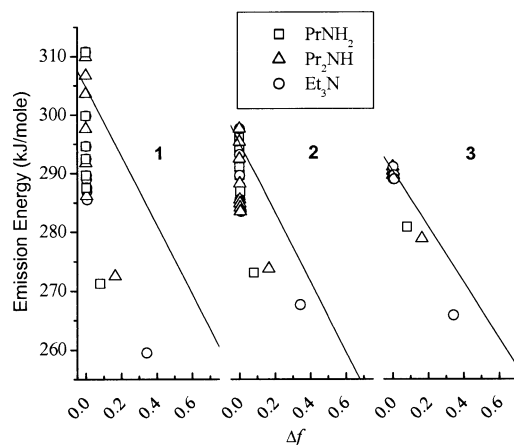


Figure 12. Emission energy for **1–3** in alkylamine–cyclohexane solutions plotted against linear Lippert–Mataga plots for pure solvents of identical bulk polarity. Without solvent–solute specific interaction or preferential solvation, the data would be expected to lie on linear Lippert–Mataga plots.

fluorescence maximum. This shift might result from preferential solvation rather than exciplex/triplex formation.

In binary solvents, an equilibrium is reached in which the entropy of solvent demixing (ΔS) is balanced with the energy of stabilization of the solute dipole (ΔE , eq 10). For ideal solutions, i.e., those that obey eq 11, eq 12

$$\frac{d(\Delta E)}{dF} - T \frac{d(\Delta S)}{dF} = 0 \quad (10)$$

$$\Delta F_{\text{bulk}} = a\Delta F_p + b\Delta F_n \quad (11)$$

where

$$\Delta F_x = \left(\frac{\epsilon - 1}{\epsilon + 2} \right) \left(\frac{n^2 - 1}{n^2 + 2} \right)$$

$$\frac{1}{\Delta(\Delta U)} = \frac{2a^3}{\mu^2 \Delta F_{p-n}} \left[1 + \frac{x_n}{x_p} e^{-Z_{ps}} \right] \quad (12)$$

describes the effect of dielectric enrichment on a polar fluorophore,⁴² where $\Delta(\Delta U)$ is the emission energy difference between cyclohexane and the cyclohexane–amine mixture, a is the aminostilbene solute spherical cavity radius, μ is the solute dipole moment, ΔF_{p-n} is the difference between the cyclohexane and amine polarities, x_n/x_p is the bulk mole ratio of cyclohexane to amine, and Z_{ps} is the empirical index of preferential solvation. A plot of $1/\Delta(\Delta U)$ versus x_n/x_p is predicted to be linear. However, deviation from linearity indicates a solute–solvent specific interaction.⁴² Thus, upon verification of the solvent mixture ideality, via dielectric constant and refractive index measurements, eq 12 may be utilized to ascertain the nature of the solute–solvent interaction.

It was found that the measured bulk dielectric constants of the mixtures varied linearly versus mole fraction of amine and thus the bulk solvents obey eq 11 (Figure 13). Using the method of Katrib and Janini,⁴³ the solvent dielectric constant and refractive index measurements yielded dipole moments of the amines that agree well with published values, 1.24, 0.98, and 0.77 for PrNH_2 , Pr_2NH , and Et_3N , respectively.⁴⁴

Assuming a dielectric enrichment model for the aminostilbene–alkylamine–cyclohexane system, plots of $1/\Delta(\Delta U)$ versus x_n/x_p should be linear. Plots for **1–3** with PrNH_2 , Pr_2NH , and Et_3N , are shown in Figure 14. No linearity is observed, from

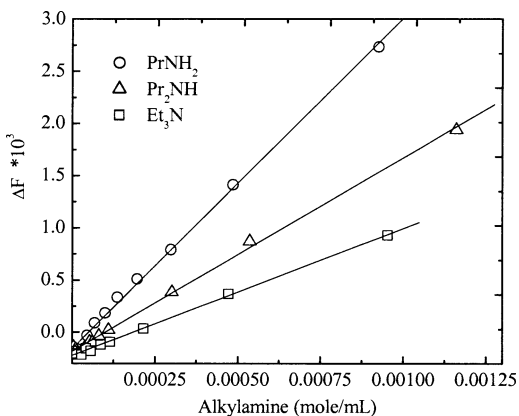


Figure 13. Plot of measured solvent polarities ΔF versus alkylamine concentration.

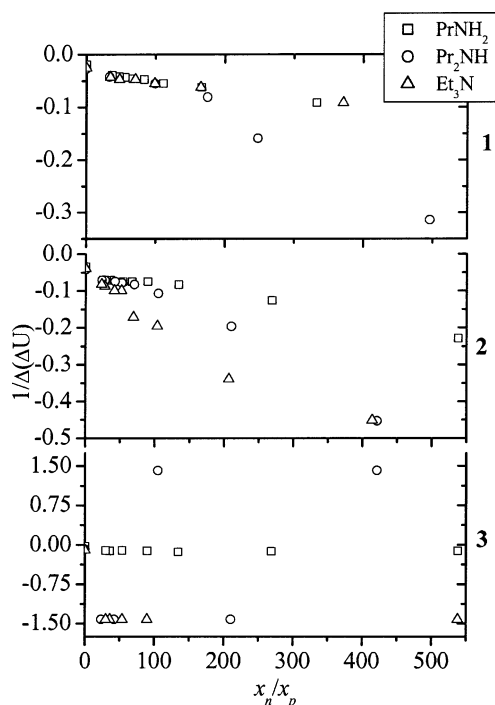


Figure 14. Inverse energy change versus solvent mole fraction for 1–3 in PrNH_2 , Pr_2NH , and Et_3N .

which it is clear that the traditional general solvent models do not adequately account for the observed interaction of the excited state aminostilbenes and the ground state amines in nonpolar solvents.

Concluding Remarks

Interaction of the singlet state of the 3-aminostilbenes with aliphatic amines results in the sequential formation of fluorescent stoichiometric 1:1 and 1:2 complexes. Complex formation is attributed to the interaction of the polar singlet state in which the electron deficient amine serves as a lone pair acceptor and the ground state amines serve as lone pair donors, resulting in the formation of a two-center three-electron bond. These observations are analogous to those reported by Chandross^{9,13} for quenching of the intramolecular naphthalene–tertiary amine exciplex and CT singlet state of 9-(4-(dimethylamino)phenyl)-anthracene by low concentrations of small polar molecules such as dimethylformamide in methylcyclohexane solution. The observation of continuously shifting emission with increasing DMF concentration was attributed to the formation of 1:1 and

1:2 complexes with lone pair donor–acceptor character; however, methods were not readily available at that time for the deconvolution of the spectra and kinetic analysis.

The quenching of fluorescent arene–trialkylamine exciplexes^{12,13,15} and the ICT states of molecules such as (dimethylamino)benzoxonitrile^{7,13} by ground state amines has also previously been attributed to lone pair donor–acceptor interactions; however, no shifted fluorescence was reported in these cases. In view of the small red shifts that we observe upon addition of amines to **3**, the stabilization of these exciplexes and ICT states upon LAB triplex formation may be too small to result in an observable red shift in their fluorescence maxima. It should, however, be possible to observe the formation of LAB exciplexes and triplexes upon interaction of the fluorescent singlet states of other primary and secondary aminoarenes with ground state amines. We report elsewhere an investigation of 9-aminophenanthrene and several of its derivatives, which suggests that this is indeed the case.⁴⁵

Acknowledgment. Funding for this project was provided by NSF grant CHE-0100596.

Supporting Information Available: 500 MHz ¹H NMR of **1–5** in CDCl_3 at 298 K. This material is available free of charge via the Internet at <http://pubs.acs.org>.

References and Notes

- (1) Lewis, F. D. Photoaddition Reactions of Amines with Aryl Olefins and Arenes. In *Advances in Electron-Transfer Chemistry*; Mariano, P. S., Ed.; JAI Press Inc.: London, 1996; Vol. 5, pp 1; Lewis, F. D. *Acc. Chem. Res.* **1979**, *12*, 152.
- (2) Chandross, E. A.; Thomas, H. T. *Chem. Phys. Lett.* **1971**, *9*, 393. Lewis, F. D.; Ho, T.-I. *J. Am. Chem. Soc.* **1977**, *99*, 7991. Lewis, F. D.; Bassani, D. M.; Burch, E. L.; Cohen, B. E.; Engleman, J. A.; Reddy, G. D.; Schneider, S.; Jaeger, W.; Gedeck, P.; Gahr, M. *J. Am. Chem. Soc.* **1995**, *117*, 660.
- (3) Kuzmin, M. G.; Guseva, L. N. *Chem. Phys. Lett.* **1969**, *3*, 71. Davidson, R. S.; Trethewey, K. R. *J. Chem. Soc. Chem. Commun.* **1976**, 827. Yang, N. C.; Libman, J. *J. Am. Chem. Soc.* **1973**, *95*, 5783. Okada, T.; Mori, T.; Mataga, N. *Bull. Chem. Soc. Jpn.* **1976**, *49*, 3398. Van, S.-P.; Hammond, G. S. *J. Am. Chem. Soc.* **1978**, *100*, 3895. Jacques, P.; Haselbach, E.; Henseler, A.; Pilloud, D.; Suppan, P. *J. Chem. Soc., Faraday Trans.* **1991**, *87*, 3811. Jacques, P.; Burget, D.; Allonas, X. *New J. Chem.* **1996**, *20*, 933.
- (4) Brimage, D. R. G.; Davidson, R. S. *J. Chem. Soc. D, Chem. Commun.* **1971**, 1385. Van der Auweraer, M.; Gilbert, A.; De Schryver, F. C. *J. Phys. Chem.* **1981**, *85*, 3198. Van der Auweraer, M.; Grabowski, Z. R.; Rettig, W. *J. Phys. Chem.* **1991**, *95*, 2083.
- (5) Van der Auweraer, M.; Swinnen, A. M.; De Schryver, F. C. *J. Chem. Phys.* **1982**, *77*, 4110.
- (6) Lewis, F. D.; Reddy, G. D.; Schneider, S.; Gahr, M. *J. Am. Chem. Soc.* **1991**, *113*, 3498. Lewis, F. D.; Cohen, B. E. *J. Phys. Chem.* **1994**, *98*, 10591.
- (7) Wang, Y. *Chem. Phys. Lett.* **1985**, *116*, 286. Wang, Y. *J. Chem. Soc., Faraday Trans. 2* **1988**, *84*, 1809.
- (8) Lewis, F. D.; Crompton, E. M. SET Addition of Amines to Alkenes. In *CRC Handbook of Organic Photochemistry and Photobiology*, 2nd ed.; Horspool, W., Lenci, F., Eds.; CRC Press: Boca Raton, 2003.
- (9) Chandross, E. A.; Thomas, H. T. *Chem. Phys. Lett.* **1971**, *9*, 397.
- (10) Beecroft, R. A.; Davidson, R. S.; Goodwin, D. *Tetrahedron* **1985**, *41*, 3853. Yang, N. C. C.; Minsek, D. W.; Johnson, D. G.; Larson, J. R.; Petrich, J. W.; Gerald, R.; Wasielewski, M. R. *Tetrahedron* **1989**, *45*, 4669. Salties, J.; Townsend, D. E.; Watson, B. D.; Shannon, P. *J. Am. Chem. Soc.* **1975**, *97*, 5688. Itoh, M.; Takita, N.; Matsumoto, M. *J. Am. Chem. Soc.* **1979**, *101*, 7363. Masuhara, H.; Mataga, N. *Chem. Phys. Lett.* **1973**, *22*, 305. Hirata, Y.; Takimoto, M.; Mataga, N.; Sakata, Y.; Misumi, S. *Chem. Phys. Lett.* **1982**, *92*, 76. Beens, H.; Weller, A. *Chem. Phys. Lett.* **1968**, *2*, 140. Grellmann, K. H.; Suckow, U. *Chem. Phys. Lett.* **1975**, *32*, 250. Caldwell, R. A.; Creed, D.; DeMarco, D. C.; Melton, L. A.; Ohta, H.; Wine, P. H. *J. Am. Chem. Soc.* **1980**, *102*, 2369.
- (11) Fages, F.; Desvergne, J. P.; Bouas-Laurent, H. *J. Am. Chem. Soc.* **1989**, *111*, 96.
- (12) Lewis, F. D.; Bassani, D. M. *J. Photochem. Photobiol., A* **1992**, *66*, 43.

- (13) Chandross, E. A. Complexes of Dipolar Excited States and Small Polar Molecules. In *The Exciplex*; Gordon, M., Ware, W. R., Eds.; Academic Press: New York, 1975; p 372.
- (14) Burget, D.; Jacques, P.; Vauthey, E.; Suppan, P.; Haselbach, E. *J. Chem. Soc., Faraday Trans.* **1994**, *90*, 2481.
- (15) Schneider, S.; Geiselhart, P.; Seel, G.; Lewis, F. D.; Dykstra, R. E.; Nepras, M. *J. Phys. Chem.* **1989**, *93*, 3112. Hub, W.; Schneider, S.; Doerr, F.; Oxman, J. D.; Lewis, F. D. *J. Phys. Chem.* **1983**, *87*, 4351.
- (16) Lewis, F. D.; Li, L.-S.; Kurth, T. L.; Kalgutkar, R. S. *J. Am. Chem. Soc.* **2000**, *122*, 8573.
- (17) Volkov, V. V. *Appl. Spectrosc.* **1996**, *50*, 320.
- (18) Zimanyi, L.; Kulcsar, A.; Lanyi, J. K.; Sears, D. F., Jr.; Saltiel, J. *Proc. Natl. Acad. Sci. U.S.A.* **1999**, *96*, 4408. Zimanyi, L.; Kulcsar, A.; Lanyi, J. K.; Sears, D. F., Jr.; Saltiel, J. *Proc. Natl. Acad. Sci. U.S.A.* **1999**, *96*, 4414. Henry, E. R.; Hofrichter, J. *Methods Enzymol.* **1992**, *210*, 129.
- (19) Lee, B. H.; Marvel, C. S. *J. Polym. Sci., Part A: Polym. Chem.* **1982**, *20*, 393.
- (20) Taylor, T. W. J.; Hobson, P. M. *J. Chem. Soc. Abstr.* **1936**, 181.
- (21) Boyer, J. H.; Alul, H. *J. Am. Chem. Soc.* **1959**, *81*, 2136.
- (22) Haddow, A.; Harris, R. J. C.; Kon, G. A. R.; Roe, E. M. *F. Trans. R. Soc. (London)* **1948**, *A 241*, 147.
- (23) Beletskaya, I. P.; Bessmertnykh, A. G.; Guillard, R. *Tetrahedron Lett.* **1997**, *38*, 2287. Driver, M. S.; Hartwig, J. F. *J. Am. Chem. Soc.* **1996**, *118*, 7217.
- (24) Model 350G. Dielectric Products Company, 178 Orchard St. Watertown, MA 02172; phone 617-924-5688.
- (25) Breitung, E. M.; Vaughan, W. E.; McMahon, R. J. *Rev. Sci. Instrum.* **2000**, *71*, 224.
- (26) Berlman, I. B. *Handbook of Fluorescence Spectra of Aromatic Molecules*, 2nd ed.; Academic Press: New York, 1971.
- (27) James, D. R.; Siemiarczuk, A.; Ware, W. R. *Rev. Sci. Instrum.* **1992**, *63*, 1710.
- (28) Photon Technologies Incorporated, 347 Consortium Court, London, Ontario N6E 2S8, Canada.
- (29) Lewis, F. D.; Weigel, W. *J. Phys. Chem. A* **2000**, *104*, 8146.
- (30) Lewis, F. D.; Kalgutkar, R. S.; Yang, J.-S. *J. Am. Chem. Soc.* **1999**, *121*, 12045.
- (31) Rettig, W.; Bliss, B.; Dirnberger, K. *Chem. Phys. Lett.* **1999**, *305*, 8. Zaitsev, N. K.; Demyashkevich, A. B.; Kuzmin, M. G. *Russian J. Appl. Spectrosc.* **1978**, *29*, 496.
- (32) Rückert, I.; Demeter, A.; Morawski, O.; Kuehnle, W.; Tauer, E.; Zachariasse, K. A. *J. Phys. Chem. A* **1999**, *103*, 1958.
- (33) ¹H NMR also clearly indicates the small effect of methylation on geometry; see Supporting Information.
- (34) CAChe, v. 5.0; Fujitsu Limited: Mihama-Ku, Chiba City, Chiba, Japan, 2000–2001.
- (35) Lippert, E. *Z. Naturforsch.* **1955**, *10a*, 541. Liptay, W. *Z. Naturforsch.* **1965**, *20a*, 1441. Mataga, N.; Ottolenghi, M. In *Molecular Association*; Foster, R., Ed.; Academic Press: New York, 1979; Vol. 2; p 1. Mataga, N. In *Molecular Interactions*; Ratajczak, H., Orville-Thomas, W. J., Redshaw, M., Eds.; Wiley: New York, 1981; Vol. 2, p 509.
- (36) Lagarias, J. C.; Reeds, J. A.; Wright, M. H.; Wright, P. E. *SIAM J. Optim.* **1998**, *9*, 112. Shampine, L. F.; Reichelt, M. W. *SIAM J. Sci. Comput.* **1997**, *18*, 1. Gill, P. E.; Murray, W.; Wright, M. H. *Practical Optimization*; Academic Press: London; New York, 1981. Rate constants represent best-fits and errors are estimated to be $\pm 10\%$ via bracketing of solutions.
- (37) Brown, H. C.; Taylor, M. D. *J. Am. Chem. Soc.* **1947**, *69*, 1332.
- (38) Lewis, F. D.; Reddy, G. D.; Bassani, D.; Schneider, S.; Gahr, M. *J. Photochem. Photobiol., A* **1992**, *65*, 205.
- (39) Suppan, P. *J. Chem. Soc., Faraday Trans. 1* **1987**, *83*, 495.
- (40) Suppan, P.; Ghoneim, N. *Solvatochromism*; The Royal Society of Chemistry: Cambridge, U.K., 1997.
- (41) Suppan, P. *Chem. Phys. Lett.* **1983**, *94*, 272. Petrov, N. K.; Wiessner, A.; Staerk, H. *J. Chem. Phys.* **1998**, *108*, 2326.
- (42) Khajehpour, M.; Welch, C. M.; Kleiner, K. A.; Kauffman, J. F. *J. Phys. Chem. A* **2001**, *105*, 5372. Khajehpour, M.; Kauffman, J. F. *J. Phys. Chem. A* **2000**, *104*, 7151.
- (43) Janini, G. M.; Katrib, A. H. *J. Chem. Educ.* **1983**, *60*, 1087.
- (44) Lide, D. R. *CRC Handbook of Chemistry and Physics*, 82nd ed.; CRC Press: Boca Raton, FL, 2001.
- (45) Lewis, F. D.; Ahrens, A.; Kurth, T. L. *Photochem. Photobiol. Sci.*, in press.